# Communication—Lithium Titanate as Mg-Ion Insertion Anode for Mg-Ion Sulfur Batteries Based on Sulfurated Poly(acrylonitrile) Composite

View the article online for updates and enhancements.

CrossMark

# Communication—Lithium Titanate as Mg-Ion Insertion Anode for Mg-Ion Sulfur Batteries Based on Sulfurated Poly(acrylonitrile) Composite

Janina Trück,[1,2] Peiwen Wang,[1] Elizaveta Buch,[2] Jonas Groos,[1] Stefan Niesen,[1,2] and Michael R. Buchmeiser[1,3,z] (ORCID)

[1]*Institute of Polymer Chemistry, University of Stuttgart, 70569 Stuttgart, Germany*
[2]*RD/EBZ, Daimler AG, 70327 Stuttgart, Germany*
[3]*German Institute of Textile and Fiber Research (DITF), 73770 Denkendorf, Germany*

Spinel lithium-titanate $Li_4Ti_5O_{12}$ (LTO) is a promising anode material for magnesium batteries due to its non-toxicity, low-cost, zero-strain characteristics and long-term stability. Nevertheless, the application of LTO in a magnesium full cell has been rarely investigated. Herein, we give a proof of concept for the feasibility of LTO as anode in full magnesium ion batteries, which might prevent the passivation of metallic Mg anodes. $Mg^{2+}$ was electrochemically inserted into LTO prior to cycling against a sulfur-based cathode material, i.e. sulfurated poly(acrylonitrile), SPAN, resulting in stable cycle performance with 800 mAh $g_S^{-1}$ at 0.3C and high-rate capability.
© 2022 The Electrochemical Society ("ECS"). Published on behalf of ECS by IOP Publishing Limited. [DOI: 10.1149/1945-7111/ac4547]

Rechargeable magnesium batteries are of increasing interest, since the drawbacks of lithium-ion batteries (high costs, use of rare elements, low theoretical energy density) become more crucial with the growing demand for energy storage devices. In this context, Aurbach et al. reported the first rechargeable Mg battery prototype.[1] Especially the combination with sulfur-based cathodes is promising as the cells possess high theoretical volumetric capacity (3832 mAh $cm^{-3}$) and both Mg and S are highly abundant, save and non-toxic.[2]

Literature on anodes mainly focusses on metallic Mg as foils or high-surface, pressed Mg powders.[2–4] In sharp contrast, reports on insertion- or conversion-type anode materials for Mg-S batteries are still rare.[2,5] Since metallic Mg is prone to form a blocking layer in most common electrolytes, the development of $Mg^{2+}$ insertion anodes is crucial.[6] These should be compatible with simple Mg salts and solvents with wider electrochemical stability enabling more feasible systems.[7]

$Li_4Ti_5O_{12}$ (LTO) is a low-cost, non-toxic and abundant lithium-insertion anode material known for its high stability and zero-strain characteristics,[8,9] which also applies for $Mg^{2+}$ insertion/extraction.[10] However, the poor electronic conductivity of the material and the slow ionic diffusion of $Mg^{2+}$ are severely limiting performance. Several approaches to overcome this obstacle have been reported in the literature; these include particle size reduction, carbon coating or doping.[11–13] However, the most effective strategy to substantially improve the electrochemical performance is reported to be the combined lithiation and magnesiation of LTO by using a $Mg^{2+}/Li^+$ dual salt electrolyte.[12,14]

There is a deep understanding of the mechanisms during $Mg^{2+}/Li^+$ co-insertion into LTO,[10,14] however, investigations on LTO as anode material for full Mg-ion batteries (MIBs) are still lacking. Here, we demonstrate the feasibility of a full-cell utilizing an electrochemically pre-magnesiated LTO anode, a dual salt electrolyte and a sulfurated poly(acrylonitrile) ("SPAN") cathode.[15–19] Li-ions in the dual salt electrolyte reduce the resistance, the overpotential and improve the reaction kinetics of Mg-cells with SPAN.[19] This work provides a proof of concept for the feasible application of LTO as anode in full MIBs.

## Experimental

***Chemicals.***—All samples were handled in an Ar-filled glovebox ($c_{oxygen} < 0.1$ ppm, $c_{water} < 0.1$ ppm). PAN, sulfur, anhydrous

1,2-dimethoxyethane (DME, 99.5%), lithium carbonate ($Li_2CO_3$) and titanium dioxide ($TiO_2$) were purchased from Merck and used as received. Magnesium trifluoromethanesulfonate ($Mg(CF_3SO_3)_2$), magnesium chloride ($MgCl_2$), aluminum chloride ($AlCl_3$) and lithium trifluoromethanesulfonate ($Li(CF_3SO_3)$) were purchased from Merck and dried at 120 °C. Mg and graphite foils were purchased from Advent Research Materials and Alfa Aesar Germany, respectively, and punched into discs (Ø 12 mm). Mg chips were polished with a ceramic knife in a glovebox to remove the oxide layer before cell-assembling.

***Electrolyte.***—0.2 M $Mg(CF_3SO_3)_2$, 0.4 M $MgCl_2$, 0.4 M $AlCl_3$ and 1.6 M $Li(CF_3SO_3)$ were consecutively added to dry DME[19] and the resulting mixture was stirred overnight at room temperature. The electroactive species in this system is $[Mg_2(\mu_2\text{-Cl})_2(DME)_4]^{2+}$.

***LTO.***—LTO was prepared via a mixed oxide route from $Li_2CO_3$ and $TiO_2$. They were first mixed in a stoichiometric ratio in isopropanol. Afterwards, they were dried using a rotary evaporator, then further at 80 °C under vacuum overnight and calcined in air in two steps: first at 400 °C for 8 h, then at 800 °C for 12 h.[20] Finally, the powder was milled in isopropanol in an attritor for 6 h at 1000 rpm with active water cooling.

***SPAN.***—Particulate sulfurated-poly(acrylonitrile) (SPAN) was prepared according to the literature.[21] The obtained SPAN compound was dried *in vacuo* overnight, ground and sieved below 63 $\mu$m. Elemental analysis of SPAN: C, 44.08%; H, 1.048%; N, 13.66%; S, 38.32%.

***LTO electrodes.***—The LTO slurry comprised LTO, carbon black and PVDF in a weight ratio of 8:1:1 and NMP (NMP:LTO = 2.5:1). The slurry was mixed at 2,000 rpm in a *Thinky* (ARE-310) and coated on a carbon coated Al-foil with a wet thickness of 300 $\mu$m by doctor blading. After drying, NMP was removed at 60 °C overnight. The average areal capacity was 1.2 mAh $cm^{-2}$.

***SPAN cathodes.***—The cathode slurry comprised SPAN, carbon black and PVDF in a the weight ratio of 70:15:15 and NMP (NMP: SPAN = 10:1). The slurry was mixed at 2,000 rpm in a *Thinky* and coated on the graphite foils by spin coating and dried at 60 °C overnight. For an anode excess of ca. 50%, the average areal capacity was set to 0.8 mAh $cm^{-2}$.

[z]E-mail: michael.buchmeiser@ipoc.uni-stuttgart.de
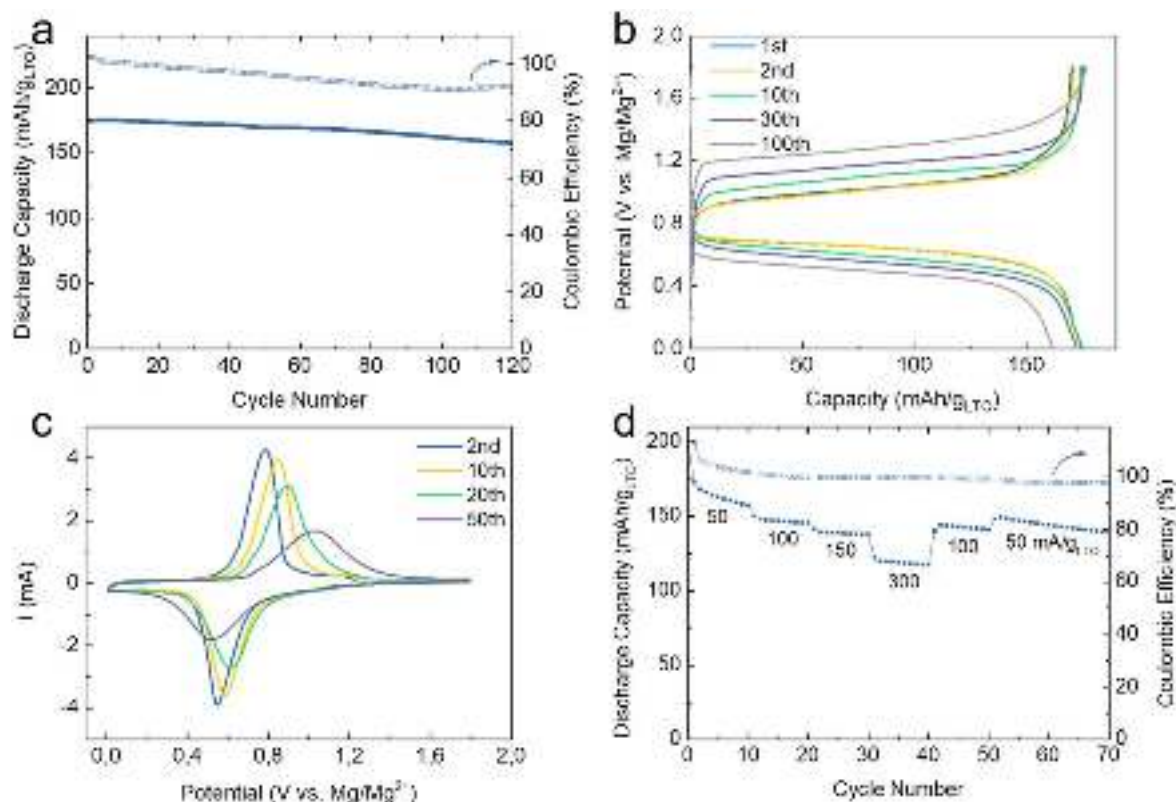
**Figure 1.** (a): Capacity retention of Mg-LTO half-cells at 150 mA $g_{LTO}^{-1}$; (b): Typical charge-discharge curves of Mg-LTO half-cells at 150 mA $g_{LTO}^{-1}$; (c): Cyclic voltammogram of a Mg-LTO half-cell at a scan rate of 0.2 mV $s^{-1}$; (d): Rate test between 50 and 300 mA $g_{LTO}^{-1}$.

*Electrochemistry.*—For half-cell cycling and overpotential measurements two electrode cells (T-cells, Swagelok) and for full-cell cycling and cyclic voltammetry (CV) three electrode PAT-cells (EL-cell) were utilized. The half-cells comprised Mg foil (Ø 12 mm), LTO electrode (Ø 12 mm) and two glass fiber separators (Whatman, Ø 12.5 mm) wetted with 150 μl of electrolyte. The full-cells comprised pre-cycled LTO electrode, an SPAN cathode, a Mg reference electrode and one glass fiber separator wetted with 120 μl of electrolyte. Cycling data of the half-cells were recorded on a BasyTec XCTS-LAB system at 0.01–1.8 V vs Mg/Mg$^{2+}$. Cycling data of the full-cells were recorded by EC-Lab at 0.1–2 V vs Mg/Mg$^{2+}$.

*Materials characterization.*—SEM/EDX was measured on a Auriga type field emission scanning electron microscope (Zeiss). XRD was measured on a Stoe Stadi P (Stoe GmbH&Cie, Mo source: λ = 70.93 pm). For ICP-OES, the particulate anode materials were dissolved in $H_2O_2/H_2SO_4$; full dissolution was ensured by microwave heating. The measurements were carried out on a SPECTRO ARCOS FH16 spectrometer and the software Smart Analyzer. Mg was measured at λ = 285.213 nm (background 285.130–285.156 and 285.312–285.332 nm).

### Results and Discussion

Figure S1 (S.I.) (available online at stacks.iop.org/JES/169/010505/mmedia) shows the morphology of the prepared LTO particles with the primary particles being in the range of 200–600 nm and agglomerates in the μm range. Compared to the literature on Mg$^{2+}$ insertion into LTO, these are amongst the largest particles reported so far.[10,11,14,22] However, in contrast to the sol-gel attempts dominating the literature, the synthetic route outlined here is straightforward, easily scalable and therefore beneficial for further research, upscaling and potential future application. The corresponding X-ray diffraction (XRD) pattern of LTO is shown in

Fig. S2 (S.I.). It confirms the presence of the face-centered cubic spinel type $Li_4Ti_5O_{12}$ crystal structure.[23] In addition, an energy dispersive X-ray spectroscopy measurement (EDX) is given in Fig. S3 (S.I.) to confirm the absence of impurities.

Next, the electrochemical performance of the Mg-ion insertion into LTO was investigated in half-cells with Mg foil as counter electrode. The current rate was 150 mA $g_{LTO}^{-1}$ (1C = 175 mA $g^{-1}$, according to the theoretical capacity of LTO). Figure 1a shows the high discharge capacity of ca. 170 mAh$g_{LTO}^{-1}$ and the good reversibility with 90%capacity retention after 120 cycles (175 to 157 mAh $g_{LTO}^{-1}$).

The charge-discharge curves display the characteristic flat plateaus of the Mg$^{2+}$ insertion in LTO (Fig. 1b). The onsets of the voltage plateaus for the charge and discharge in the first cycle were at 0.9 V and 0.7 V, respectively, and shifted continuously to 1.2 V and 0.6 V, respectively. The increasing voltage gap is attributed to a polarization of the electrode and may explain the capacity decay observed in the cycle test. In order to further understand the system, three-electrode cells with a Mg-reference were fabricated. CV showed one reduction and one oxidation peak as expected (Fig. 1c). The high current observed is indicative for the effectiveness of the redox process. The onsets of the peaks are in accordance with the plateaus of the charge-discharge curves.

In the rate-capability test (Fig. 1d), the half-cell shows stable behavior and outstanding high capacity of 120 mAh $g_{LTO}^{-1}$ at 300 mA $g_{LTO}^{-1}$, which performs better than the reported nonosized LTO.[14] This confirms the practicability of our facile solid-state synthesis route.

In order to prove the insertion of Mg$^{2+}$ into the LTO structure, *post-mortem* measurements of the electrodes via inductively-coupled plasma-optical emission spectroscopy (ICP-OES) were conducted. Mg-LTO half-cells were disassembled after cycling and washed thoroughly to remove residual electrolyte. Already after the initial discharge, 0.04 mol% of Mg were found in the LTO, which indicates the successful insertion of Mg. Further confirmation was provided by EDX measurements (Fig. S4, S.I.). The high intensity of the Mg
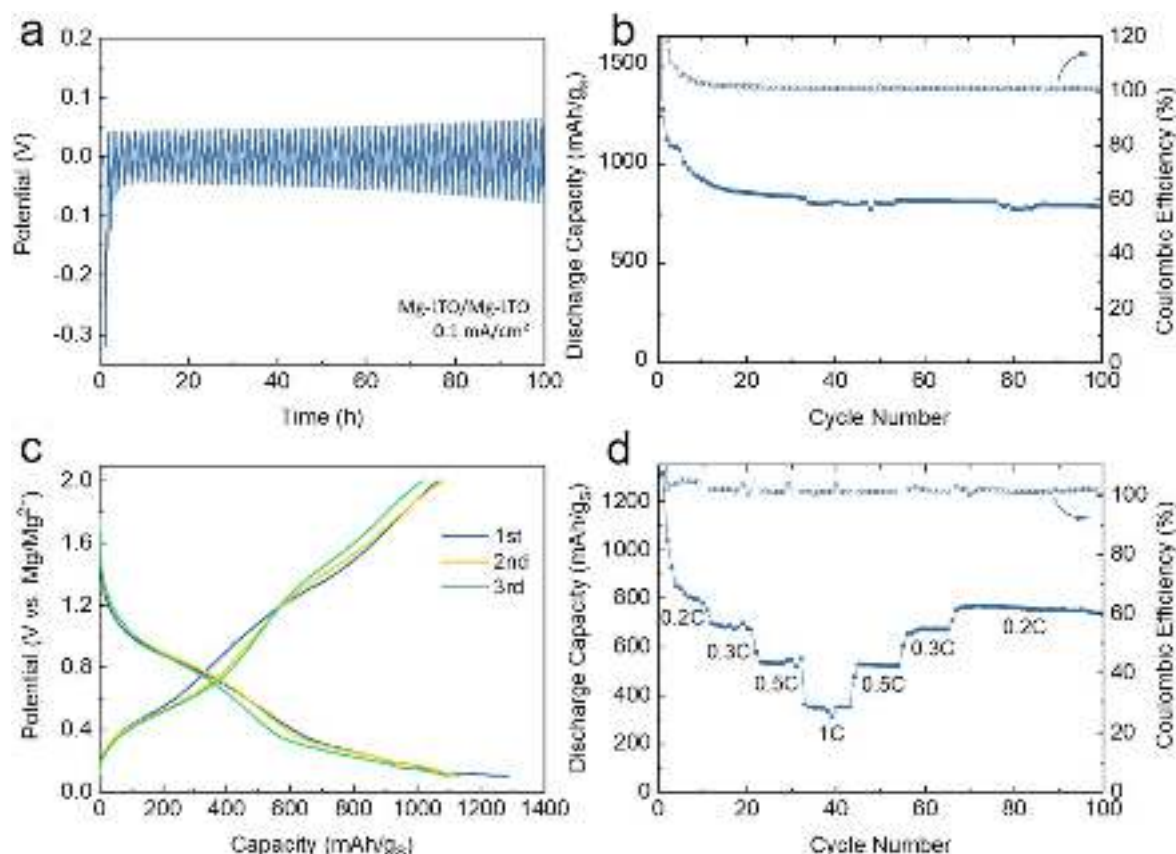
**Figure 2.** (a): Overpotential measurement of LTO symmetric cells at 0.1 mA cm$^{-1}$. The LTO electrodes were equally pre-cycled in Mg-LTO half-cells to partly insert Mg; (b): Cycle stability of LTO-SPAN full-cells at 0.3C; (c): Typical charge-discharge curves of LTO-SPAN full-cells at 0.3C; Rate test of LTO-SPAN full-cell between 0.2 and 1C.

signal is a valid sign for the presence of Mg in the LTO. While F is present in the electrode-binder (PVDF), the other residuals are most probably attributable to an interface layer formed during cycling (Al, Cl, S) and the glass fiber separator (Na, Si). Mg might also be part of the interface layer. However, due to the comparably low concentration of Mg in the electrolyte, the high intensity of the Mg signal is a valid sign for the presence of Mg in the LTO. In addition, LTO vs Mg cycling in 1.6 M Li(SO$_3$CF$_3$) electrolyte showed no capacity ($< 1$ mAh/g$_{LTO}$).

In order to assess the suitability of the electrolyte, symmetric LTO-LTO cells were used to evaluate the overpotential of the Mg$^{2+}$ insertion/extraction reaction process. Prior to measurements, the LTO electrodes were equally pre-cycled against Mg-foil to store Mg partly in the electrodes. Results shown in Fig. 2a prove the efficiency of the electrolyte for Mg$^{2+}$ insertion/extraction and confirm the good cycle stability. In the first cycles, the overpotential is well below 0.05 V, which is low compared to the overpotential of Mg-foil electrodes in the same electrolyte.[19] The slight increase of the overpotential with time is in accordance with the previously observed polarization of the electrodes. Encouraged by these results, we accomplished a proof of concept for the practicability of LTO as insertion anode for MIBs by combining LTO with an SPAN cathode. Figure 2b shows the cycling performance of a full-cell comprising an SPAN cathode and pre-cycled LTO. The initial discharge capacity was as high as 2200 mAh g$_S^{-1}$, which is characteristic for SPAN. However, the capacity decreases to 800 mAh g$_S^{-1}$ (387 mWh g$_S^{-1}$) within the first 20 cycles but then remained constant for over 100 cycles. Research is still ongoing to optimize the energy density. Also, the Coulombic Efficiency remained stable at ca 100% after

10 cycles, indicating good reversibility of the full-cell. Complementary, different numbers of cycles for the pre-cycling in the half-cell were evaluated (Fig. S5, S.I.).

The charge-discharge curves of the full-cells are depicted in Fig. 2c. Obviously, the characteristic flat voltage plateau of the Mg$^{2+}$ insertion into LTO vanished. Instead, the sloped curve accounts for an SPAN-Mg conversion reaction. Figure S6 (S.I.) shows that the plateaus of LTO-SPAN are slightly lower compared to those in Mg-SPAN cells. According to the literature, the slope starting below 1.5 V vs Mg/Mg$^{2+}$ indicates the absence of long chain polysulfides.[15,16,18,24,25]

A test-cell containing pristine LTO and SPAN electrodes showed almost no capacity during galvanostatic cycling (Fig. S7, S.I.). This proves that the capacity of the full-cell was mainly caused by the conversion reaction of Mg from the pre-magnesiated LTO anode with SPAN and excludes any capacity contribution of the Li-ions from the electrolyte. Another test-cell of pre-cycled LTO vs SPAN with 1.6 M Li(SO$_3$CF$_3$) electrolyte suggest that 100 mAh g$_S^{-1}$ of the total capacity are attributed to the contribution of Li$^+$ co-inserted in LTO during pre-cycling.

For the evaluation of the rate capability of the novel Mg-ion/sulfur battery, a rate-test was conducted. Excellent behavior with stable capacity even at a high rate of 1C (360 mAh g$_S^{-1}$) was observed. Also, outstanding reversibility was demonstrated since the capacity returned to 800 mAh g$_S^{-1}$ at 0.2C after cycling at higher rates. This indicates once more the low-strain properties of the LTO and its suitability as anode material for MIBs, which is intended to encourage further research on combinations of LTO anodes with different cathodes and electrolytes.

## Summary

In conclusion, LTO prepared by a facile and scalable solid-state synthesis shows stable electrochemical performance in half-cells with a dual $Mg^{2+}/Li^+$ electrolyte of up to 120 mAh $g_{LTO}^{-1}$ at 300 mA $g_{LTO}^{-1}$. The feasibility of LTO as anode for magnesium-ion/sulfur batteries was successfully demonstrated using SPAN as cathode. It delivered a stable capacity of 800 mAh $g_S^{-1}$ at 0.3C and showed high rate capability with 360 mAh $g_S^{-1}$ at 1C.

## Acknowledgments

## ORCID

Michael R. Buchmeiser https://orcid.org/0000-0001-6472-5156

## References

1. D. Aurbach, Z. Lu, A. Schechter, Y. Gofer, H. Gizbar, R. Turgeman, Y. Cohen, M. Moshkovich, and E. Levi, *Nature*, **407**, 724 (2000).
2. P. Wang and M. R. Buchmeiser, *Adv. Funct. Mater.*, **29**, 1905248 (2019).
3. Z. Meng, D. Foix, N. Brun, R. Dedryvère, L. Stievano, M. Morcrette, and R. Berthelot, *ACS Energy Lett.*, **4**, 2040 (2019).
4. L. Kong, C. Yan, J.-Q. Huang, M.-Q. Zhao, M.-M. Titirici, R. Xiang, and Q. Zhang, *Energy Environ. Mater.*, **1**, 100 (2018).
5. J. Trück, P. Wang, S. Niesen, J. Kappler, K. Küster, U. Starke, F. Ziegler, A. Hintennach, and M. R. Buchmeiser, *Batteries & Supercaps*, **3**, 1239 (2020).
6. Z.-K. Zhirong and F. Maximilian, *MRS Comm.*, **7**, 770 (2017).
7. P. Saha, M. K. Datta, O. I. Velikokhatnyi, A. Manivannan, D. Alman, and P. N. Kumta, *Prog. Mater Sci.*, **66**, 1 (2014).
8. H. Liu et al., *ACS Mater. Lett.*, **1**, 96 (2019).
9. A. Wei, W. Li, L. Zhang, B. Ren, X. Bai, and Z. Liu, *Solid State Ion.*, **311**, 98 (2017).
10. N. Wu, Y.-C. Lyu, R.-J. Xiao, X. Yu, Y.-X. Yin, X.-Q. Yang, H. Li, L. Gu, and Y.-G. Guo, *NPG Asia Mater.*, **6**, e120 (2014).
11. N. Wu, Y. X. Yin, and Y. G. Guo, *Asian J. Chem.*, **9**, 2099 (2014).
12. Q. Miao, Y. NuLi, N. Wang, J. Yang, J. Wang, and S.-I. Hirano, *RSC Adv.*, **6**, 3231 (2016).
13. B. Lee, E. Jo, J. Choi, J. H. Kim, W. Chang, S. Yu, H.-S. Kim, and S. H. Oh, *J. Mater. Chem. A*, **7**, 25619 (2019).
14. N. Wu, Z. Z. Yang, H. R. Yao, Y. X. Yin, L. Gu, and Y. G. Guo, *Angew. Chem. Int. Ed.*, **54**, 5757 (2015).
15. J. Fanous, M. Wegner, J. Grimminger, Ä. Andresen, and M. R. Buchmeiser, *Chem. Mater.*, **23**, 5024 (2011).
16. J. Fanous, M. Wegner, J. Grimminger, M. Rolff, M. Spera, M. Tenzer, and M. Buchmeiser, *J. Mater. Chem.*, **22**, 23240 (2012).
17. R. Mukkabla and M. R. Buchmeiser, *J. Mater. Chem. A*, **8**, 5379 (2020).
18. J. Fanous, M. Wegner, M. Spera, and M. Buchmeiser, *J. Electrochem. Soc.*, **160**, A1169 (2013).
19. P. Wang, K. Küster, U. Starke, C. Liang, R. Niewa, and M. R. Buchmeiser, *J. Power Sources*, **515**, 230604 (2021).
20. Y. Shen, M. Søndergaard, M. Christensen, S. Birgisson, and B. B. Iversen, *Chem. Mater.*, **26**, 3679 (2014).
21. T. Lebherz, D. L. Weldin, A. Hintennach, and M. R. Buchmeiser, *Macromol. Chem. Phys.*, **221**, 1900436 (2019).
22. M. Cabello, G. F. Ortiz, P. Lavela, and J. L. Tirado, *J. Nanomater.*, **9**, 484 (2019).
23. A. S. Prakash, P. Manikandan, K. Ramesha, M. Sathiya, J. M. Tarascon, and A. K. Shukla, *Chem. Mater.*, **22**, 2857 (2010).
24. Z. Zhao-Karger et al., *ACS Energy Lett.*, **3**, 2005 (2018).
25. L. Wang, X. He, J. Li, M. Chen, J. Gao, and C. Jiang, *Electrochim. Acta*, **72**, 114 (2012).